{001} facets dominated anatase TiO₂: Morphology, formation/etching mechanisms and performance

ZHANG HaiMin[1], LIU XiaoLu[1], LI YiBing[1], LI Ying[3] & ZHAO HuiJun[1,2*]

[1]Centre for Clean Environment and Energy, and Griffith School of Environment, Griffith University, Gold Coast Campus, QLD 4222, Australia
[2]Key Laboratory of Materials Physics, Hefei Key Laboratory of Nanomaterials and Nanotechnology, Institutes of Solid State Physics, Chinese Academy of Sciences, Hefei 230031, China
[3]School of Materials Science and Engineering, Shanghai University, Shanghai 200072, China

Controllable growth of anatase TiO₂ crystals with exposed high reactive crystal facets has aroused great attention in the fields of science and technology due to their unique structure-dependent properties. Recently, much effort has been paid to synthesize anatase TiO₂ crystals with exposed high reactive {001} facets. Herein, we review the recent progress in synthesizing {001} facets dominated anatase TiO₂ crystals with different morphologies by various synthetic methods. Furthermore, our review is mainly focused on the formation/etching mechanisms of {001} facets dominated anatase TiO₂ crystals based on our and other studies. The extensive application potentials of the anatase TiO₂ crystals with exposed {001} facets have been summarized in this review such as photocatalysis, photoelectrocatalysis, solar energy conversion, lithium ion battery, and hydrogen generation. Based on the current studies, we give some perspectives on the research topic.   We believe that this comprehensive review on anatase TiO₂ crystals with high reactive {001} facets can further promote the relative research in this field.

anatase TiO₂, high reactive {001} facets, crystal growth, formation/etching mechanisms, hydrothermal synthesis

1   Introduction

Controllable growth of metallic and semi-conducting nanocrystals with high reactive facets has attracted great interest in the past decade due to their superior properties in catalysis, photocatalysis, gas sensors, photovoltaics, and lithium ion battery [1–25]. Over the past two decades, titanium dioxide (TiO₂) has been the dominant semiconductor photocatalyst owing to its superior photocatalytic activity, low cost, abundant supply, non-toxic nature and high photocorrosion resistance [26–30]. Anatase TiO₂ has exhibited excellent properties in photocatalysis and solar energy conversion due to its more negative conduction band edge potential versus rutile TiO₂ [30, 31]. However, the performance of anatase TiO₂ nanocrystals depends on not only their microstructure, size and composition, but also crystal facets [2–6, 19, 20]. For this, anatase TiO₂ nanocrystals with high reactive facets such as {001} facets are still highly desired and pursued in scientific and technological fields. But the growth of {001} facets dominated anatase TiO₂ crystals is thermodynamically unfavourable owing to their higher average surface energy (0.90 J/m²) versus that of other anatase crystal facets such as {100} (0.53 J/m²) and {101} (0.44 J/m²) [2, 32]. Therefore, development of a method able to synthesize anatase TiO₂ nanocrystals with high reactive facets (e.g., {001} facets) has become a huge challenge in scientific and technological fields. Recently, a breakthrough reported by Lu *et al.* has solved this issue [6]. Their study demonstrated that surface fluorination can dramatically decrease the {001} faceted surface energy to a level lower than that of the {101} faceted surface, and thus resulting in

*Corresponding author (email: h.zhao@griffith.edu.au)

anatase TiO$_2$ single crystals with 47% exposed {001} facets [6]. Following this breakthrough, much effort has been paid to synthesize anatase TiO$_2$ crystals with high reactive {001} facets using this surface fluorination concept, such as micrometer-sized anatase TiO$_2$ single crystals with exposed {001} facets [8, 33–37], anatase TiO$_2$ nanocrystals with exposed {001} facets [16, 18, 21, 38–45], and anatase TiO$_2$ microspheres with exposed {001} facets [7, 12, 46–49]. In this respect, several recent reviews have reported the fabrication of {001} facets dominated anatase TiO$_2$ from the point of view of synthetic strategies and crystal facet engineering control [50–52].

To date, most studies on {001} facets dominated anatase TiO$_2$ crystals mainly focus on the fabrication of anatase TiO$_2$ crystals with high percentage of exposed {001} facets [8, 12, 18, 33, 42, 43]. Mechanistically, all related reports to date have exclusively concluded that surface fluorination of anatase TiO$_2$ is responsible for lowering the {001} faceted surface energy and preserving the {001} faceted surfaces [6, 8, 12, 18, 33, 34, 42, 43]. However, this surface fluorination concept of anatase TiO$_2$ is a general conclusion. What is the key species (e.g., F$^-$ and HF) for preserving the {001} facets of anatase TiO$_2$ in the process of surface fluorination and crystal growth, which is highly concerned and critically important for understanding and controlling the growth of {001} facets dominated anatase TiO$_2$ crystals. In additional, our recent study has found that a selective etching on the {001} facets of anatase TiO$_2$ can occur under high HF concentration conditions, suggesting the reported mechanistic role of surface fluorination might be lopsided [53]. In these respects, there has been no comprehensive review insightfully illustrating and understanding the surface fluorination/etching mechanisms of {001} facets dominated anatase TiO$_2$.

Considering several recent papers have reviewed the fabrication of {001} facets dominated anatase TiO$_2$ crystals using different synthetic strategies [50–52, 54, 55], in this review, we will simply introduce the synthesis of {001} facets dominated anatase TiO$_2$ with different morphologies such as micrometer-sized single crystals, nanocrystals and microspheres. Most attention will concentrate on the mechanisms of surface fluorination and etching of {001} facets dominated anatase TiO$_2$ through theoretical and experimental studies made by our and other groups, and the performances of the {001} facets dominated anatase TiO$_2$ in many applications. We believe that this comprehensive review can add insightful knowledge for designing and controlling the growth of {001} facets dominated anatase TiO$_2$ for more extensive applications.

2 Morphology of {001} facets dominated anatase TiO$_2$ crystals

To date, {001} facets dominated anatase TiO$_2$ crystals have

been extensively fabricated by using different synthetic approaches including hydrothermal, solvothermal, nonhydrolytic solvothermal alcoholysis and gas-phase oxidation methods [6, 8, 36, 56]. Reviewing current studies on {001} facets dominated anatase TiO$_2$, the synthesized anatase crystals mainly focus on three morphologies including micrometer-sized single crystals with exposed {001} facets, microspheres with exposed {001} facets and nanocrystals with exposed {001} facets.

2.1 Micrometer-sized anatase TiO$_2$ single crystals

For micrometer-sized TiO$_2$ single crystals, improving the percentage of {001} facets is highly desired due to the high reactivity of {001} faceted surface [8, 33]. Micrometer-sized TiO$_2$ single crystals with 47% exposed {001} facets were firstly reported by Lu *et al.* in 2008 (Figure 1(a)) [6]. Subsequently, the percentage of exposed {001} facets was improved to 64% by using a water-2-propanol solvothermal synthetic approach (Figure 1(b)) [8]. By creating a fluorine rich reaction environment, Yu *et al.* fabricated successfully micrometer-sized TiO$_2$ single crystals with remarkable 80% exposed {001} facets (Figure 1(c)) [33]. Through adding H$_2$O$_2$ into hydrothermal reaction solution, micrometer-sized anatase TiO$_2$ single crystals with exposed {001} and {110} facets were successfully synthesized by Liu and co-workers, as shown in Figure 1(d) [34]. The {110} faceted surfaces have higher average surface energy (1.09 J/m^2) than that (0.90 J/m^2) of {001} faceted surfaces [2]. which may contribute the improved photocatalytic performance of the anatase TiO$_2$ single crystals [34]. These mi-
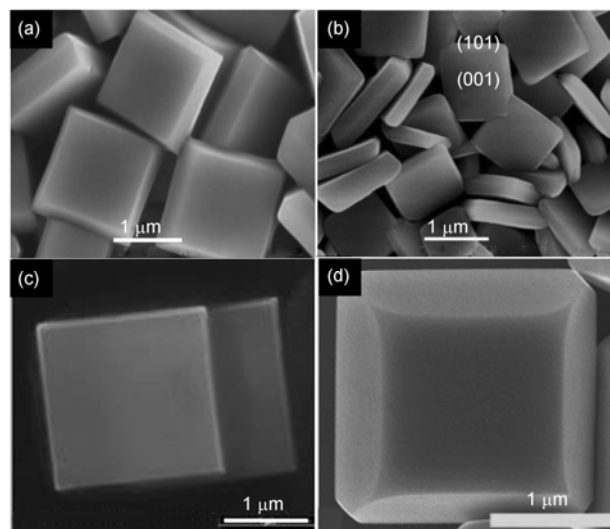

Figure 1 (a) SEM image of micrometer-sized TiO$_2$ single crystals with 47% exposed {001} facets by Lu *et al.* [6]. (b) SEM image of micrometer-sized TiO$_2$ single crystals with 64% exposed {001} facets by Lu *et al.* [8]. (c) SEM image of micrometer-sized TiO$_2$ single crystals with 80% exposed {001} facets by Yu *et al.* [33]. (d) SEM image of micrometer-sized TiO$_2$ single crystals with exposed {001} and {110} facets by Liu *et al.* [34].

crometer-sized TiO_2 single crystals with high percentage of exposed high reactive crystal facets exhibited excellent photocatalytic activity [6, 8, 33, 34].

2.2 Anatase TiO_2 microspheres with exposed {001} facets

Recently, anatase TiO_2 microspheres with exposed {001} facets have been reported by many research groups [7, 12, 46–49]. Lou and co-workers reported that anatase TiO_2 microspheres assembled from anatase nanosheets with nearly 100% exposed {001} facets can be synthesized by a facile solvothermal method [12]. Their approach mainly relies on spontaneous assembly of the anatase nanosheets into three-dimensional hierarchical microspheres with high stability, as shown in Figure 2(a) [12]. Their study further demonstrated that the anatase TiO_2 microspheres assembled from anatase nanosheets with nearly 100% exposed {001} facets exhibited superior performance in lithium ion battery [12]. Yu *et al.* reported flower-like anatase TiO_2 microspheres with exposed {001} facets using metal titanium foil as precursor by a simple hydrothermal method (Figure 2(b)) [48]. In this respect, we have developed a facile hydrothermal method to fabricate anatase TiO_2 microspheres with exposed {001} facets on metal titanium foil substrates [7, 47, 57]. The fabricated anatase TiO_2 microspheres with exposed mirror-like plane {001} facets as light harvesting enhancement material can significantly improve overall light conversion efficiency in dye-sensitized solar cells (DSSCs) [7]. More importantly, we found that the exposed crystal facets of anatase TiO_2 microspheres can happen to transform from {001} crystal facets to {101} crystal facets with hydrothermal reaction time, as shown in Figure 2(c,d)
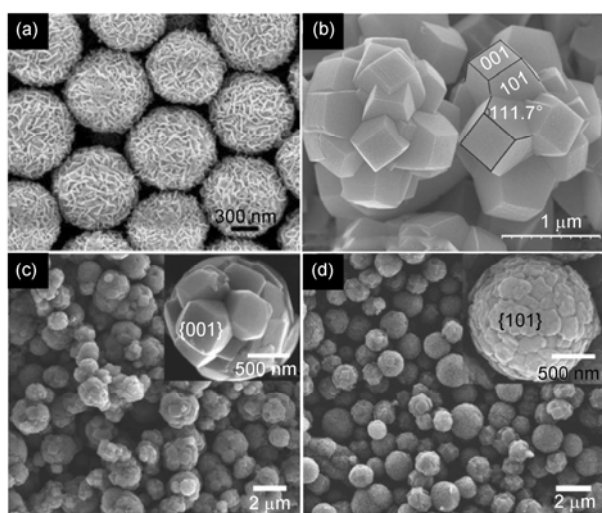

Figure 2　(a) SEM image of anatase TiO_2 microspheres assembled from anatase nanosheets with nearly 100% exposed {001} facets by Lou *et al.* [12]. (b) SEM image of anatase TiO_2 microspheres with nearly 30% exposed {001} facets by Yu *et al.* [48]. (c) and (d) SEM images of anatase TiO_2 microspheres with exposed {001} and {101} facets, respectively [47].

[47]. The photoelectrocatalytic evaluation demonstrated that the photocatalytic activity of anatase TiO_2 microspheres with exposed {001} facets was almost 1.5 times higher than that of the anatase TiO_2 microspheres with exposed {101} facets [47].

2.3 Anatase TiO_2 nanocrystals with exposed {001} facets

Although high percentage of {001} reactive facets can be reached for micrometer-sized TiO_2 single crystals, the sizes of the anatase TiO_2 single crystals are approximately micron level, which are undoubtedly too big for a number of applications that require high specific surface areas such as photocatalysis [59]. Therefore, it is highly desired to synthesize nanometer-sized anatase TiO_2 crystals with exposed {001} reactive facets [11, 16–18, 21, 38, 39, 41–45, 56, 58–60]. Wu *et al.* reported a facile nonaqueous synthetic route to fabricate anatase TiO_2 nanosheets with exposed {001} facets, as shown in Figure 3(a) [11]. Through adding appropriate amount of water to the reaction solution, high-quality rhombic-shaped anatase TiO_2 nanocrystals with a large percentage of exposed {010} facets were also obtained in their study (Figure 3(b)). The synthesized anatase TiO_2 nanosheets (or nanocrystals) with exposed {001} (or {010} facets) reactive facets shows excellent photocatalytic activity [11]. Yang and co-workers synthesized well-defined anatase TiO_2 nanosheets with 98.7% exposed {001} facets in 1-butanol solvent containing 0.2 mL of 48% HF (Figure 3(c)) [58]. They found that the formation of reaction intermediate of $TiOF_2$ is critically important for the subsequent growth of anatase TiO_2 nanosheets [58]. This finding perfects the mechanism explanation on the anatase TiO_2 nanosheets with exposed {001} facets. In the same research group, ultra-thin anatase TiO_2 nanosheets dominated with {001} reactive facets have been synthesized by a simple hydrothermal method [43]. The thickness of the anatase TiO_2 nanosheets is below 1.6 nm along [001] crystallographic direction, meaning that the nanosheets have merely two layers of anatase crystal units [43, 50]. The ultra-thin anatase TiO_2 nanosheets with exposed {001} facets exhibit high efficiency for splitting water into hydrogen under UV-vis light irradiation [43]. Combining electrospinning and hydrothermal process, Xia *et al.* synthesized successfully anatase TiO_2 nanocrystals with truncated tetragonal bipyramidal shapes and 9.6% exposed {001} facets (Figure 3(d)) [59]. They indicated that the use of electrospinning is critically important to successfully fabricate the anatase TiO_2 nanocrystals because this electrospinning approach allows for the generation of very small particles of amorphous TiO_2 to facilitate hydrothermal crystallization, an Ostwald ripening process [59]. These anatase TiO_2 nanocrystals with high reactive crystal facets could have high specific areas, and thus significantly improving their performance in photocatalysis, solar energy conversion and
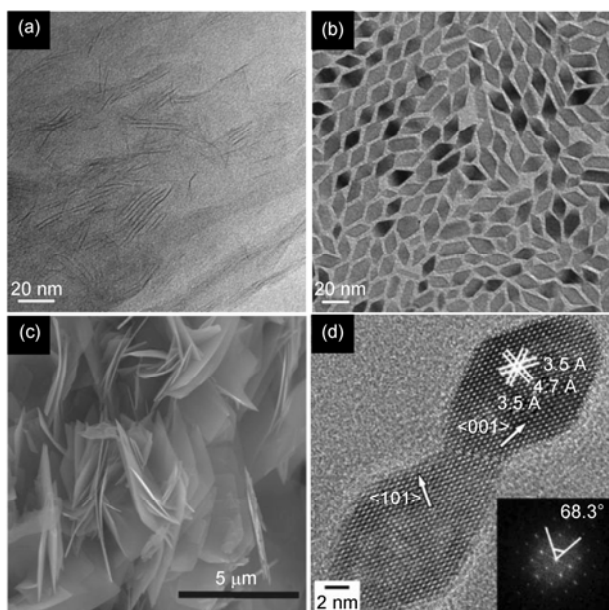
Figure 3 (a) TEM image of anatase TiO₂ nanosheets with exposed {001} facets obtained by Wu *et al.* using the nonaqueous synthetic route [11]. (b) TEM image of anatase TiO₂ nanocrystals with a large percentage of exposed {010} facets obtained by Wu *et al.* [11]. (c) SEM image of anatase TiO₂ nanosheets with 98.7% exposed {001} facets fabricated in 1-butanol solvent containing 0.2 mL of 48% HF by Yang *et al.* [58]. (d) TEM image of anatase TiO₂ nanocrystals with 9.6% exposed {001} facets by Xia *et al.* [59].

lithium ion battery [11, 16–18, 21, 38, 39, 41–45, 56, 58–60].

Overall, the {001} facets dominated anatase TiO₂ crystals with various dimensions and morphologies have different physicochemical properties, and thus exhibiting different efficacies as functional materials in applications such as photocatalysis and solar energy conversion. For large size (micron level) anatase TiO₂ crystals with exposed {001} facets, the large crystal sizes may result in low specific surface areas, which is disadvantageous for the applications that require high specific surface areas such as photocatalysis. However, the high percentage of {001} facets with high reactivity makes these single crystals able to be designed as miniature devices for more extensive applications in the future, which is highly expected.

3 Formation/etching mechanisms

As a photocatalyst, it has been extensively accepted that anatase TiO₂ is more active than rutile TiO₂ because the more negative conduction band edge potential of anatase TiO₂ than that of rutile TiO₂ is more favored to reduce O₂ to $O_2^{\cdot-}$, and thus decreasing the recombination of photoelectron and hole [27, 29, 31, 61, 62]. The superior photocatalytic properties of anatase TiO₂ can be attributed to many factors such as microstructure, size, composition, and crystal facet [6, 27, 29, 31, 50–52, 61–63]. Among these factors, high reactive crystal facets of anatase TiO₂ are still pursued in the fields of science and technology. However, high average surface energy of these crystal facets make them hard to be formed during crystal growth [2, 4]. This issue has been recently solved by Lu *et al.* through theoretical prediction and experimental confirmation [6]. Some possible crystal facets of anatase TiO₂ have been theoretically predicted and summarized in a recent review by Yang *et al.* [50]. Some crystal facets have been experimentally confirmed, while the other are expected to be realized in the future [50]. Although surface fluorination concept to date has been widely adopted to synthesize anatase TiO₂ crystals with exposed {001} facets, a question is still raised: what is the key species (e.g., F⁻ or HF) responsible for stabilizing and preserving the {001} crystal facets? Our recent finding makes the surface fluorination mechanism further clear [57]. In addition, another key issue is if the {001} crystal facets can be still preserved under any reaction conditions containing fluorine, e.g., high HF concentration solution. Our recent study has demonstrated that a selective etching on the {001} facets of anatase TiO₂ can occur under high HF concentration conditions, meaning the reported mechanistic role of surface fluorination might be lopsided [53]. Our recent findings have important guiding significance in controllable synthesis of anatase TiO₂ crystals with exposed {001} facets.

3.1 Surface fluorination

Surface chemistry of inorganic single crystals plays important role in influencing the surface stability and reactivity of single crystals, which is critically significant for the synthesis of single crystals with high reactivity [2, 3, 64–69]. For anatase TiO₂, large high reactive crystal facets (i.e., {001} facets) are difficult to be formed due to high surface energy (γ) presented by both H− and O−terminated anatase surfaces [6]. The high bonding energies (D_0) of H–H (436.0 kJ/mol) and O–O (498.4 kJ/mol) [6, 70]. Therefore, Lu *et al.* demonstrated that using a low-D_0 element with strong bonding to Ti can provide an effective means for stabilizing the surfaces [6]. By comparing various adsorbate atoms such as H, B, C, N, O, F, Si, Cl, Br, and I based on first-principle calculations, they found that F is such a element, as $D_0^{F-F} = 158.8$ kJ/mol and $D_0^{F-Ti} = 569.0$ kJ/mol, which can stabilize and preserve the anatase {001} crystal facets, as shown in Figure 4 [6, 70].

Their calculation results indicated that it is possible to obtain anatase TiO₂ single crystals with high percentage of exposed {001} facets if their surfaces are surrounded by F atoms [6]. To confirm these theoretical predictions, they synthesized experimentally anatase TiO₂ single crystals with 47% exposed {001} reactive facets (Figure 1(a)) [6]. Subsequently, anatase TiO₂ single crystals with 64% exposed {001} facets were obtained in the same research
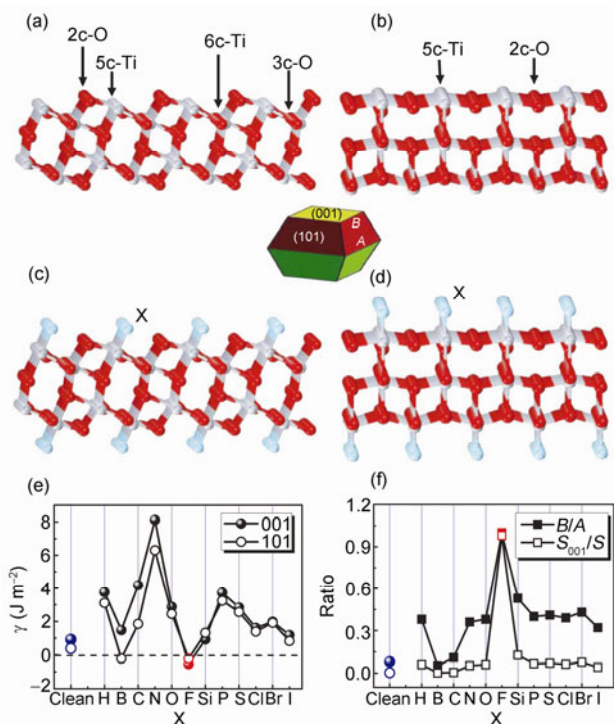
Figure 4 Slab models and calculated surface energies of anatase TiO$_2$ (001) and (101) surfaces. The optimized rations of B/A and percentage of {001} facets (S_{001}/S), where S and S_{001} are respectively the total surface area and that contributed by the {001} facets, are also shown. a, b, Unrelaxed, clean (001) and (101) surfaces. Ti and O atoms are represented by grey and red spheres, with sixfold Ti, fivefold Ti, threefold O and twofold O labelled as 6c-Ti, 5c-Ti, 3c-O and 2c-O, respectively. c, d, Unrelaxed (001) and (101) surfaces surrounded by adsorbate X atoms. e, Calculated energies of the (001) and (101) surfaces surrounded by X atoms. f, Plots of the optimized value of B/A and percentage of {001} facets for anatase single crystals with various adsorbate atoms X. In e and f, clean-surface results (denoted by blue spheres and circles) are used for reference. As indicated in the inset diagram, two independent parameters A and B denote lengths of the side of the bipyramid and the side of the square {001} 'truncation' facets, respectively. The ratio of highly reactive {001} facets to total surface area may therefore be described by the value of S_{001}/S or B/A (where $0 \leq B/A \leq 1$) by Lu *et al.* [6].

group (Figure 1(b)) [8]. The high percentage of exposed {001} facets of anatase TiO$_2$ is attributed to the added 2-propanol strengthening the stabilization effect associated with fluorine adsorption over (001) surface, and thus stimulating its preferred growth [8]. To date, all reported experimental data and theoretical calculation results have demonstrated that a fluorine rich crystal surface is essential for stabilization and preservation of {001} facets during crystal growth [6, 8, 18, 33]. Moreover, this fluorine rich crystal surface environment can only be obtained under acidic conditions [6, 8, 18, 33]. This means that pH of a reaction medium may play an important role in determining the surface fluorination, and thus the size of exposed {001} facets of anatase TiO$_2$ [57]. Although surface fluorination concept has been used as a guide to synthesize various anatase TiO$_2$ crystals with high reactive {001} facets [50–52], the mechanistic aspects, especially the preferential adsorption species

(e.g., HF molecule or F$^-$ in HF reaction solution) on {001} faceted surfaces, and the relationship between adsorption amount and surface area of exposed {001} facets remain elusive. Our recent study has indicated that the pH of reaction medium containing fluorine has significant influence on the size of exposed {001} facets of anatase TiO$_2$ [57]. This effect has been explained very well by theoretical calculations and experimental results [57]. More importantly, our study makes the surface fluorination mechanism of anatase TiO$_2$ for preserving {001} crystal facets more clear.

3.2 Mechanistic role of hydrofluoric acid (HF)

Using HF reaction medium, we found that controlling solution pH can not only control the morphology, crystal phase and composition of resultant hydrothermal products, but also control the size of exposed {001} facets of anatase TiO$_2$ crystals below pH 5.8, as shown in Figure 5(a). In a real HF reaction medium with different pHs, the possible adsorption species could include HF, F$^-$, H$^+$ and Na$^+$ (Na$^+$ originated from NaOH for solution pH adjustment). Due to the strong H−F bonding energy (D_0 = 5.91 eV) [71], HF is a weak acid (pKa = 3.17), which means that the HF molecule and Na$^+$F$^-$ will be the dominant species at low and high pHs, respectively (Figure 5(b)) [57]. Using first principle density
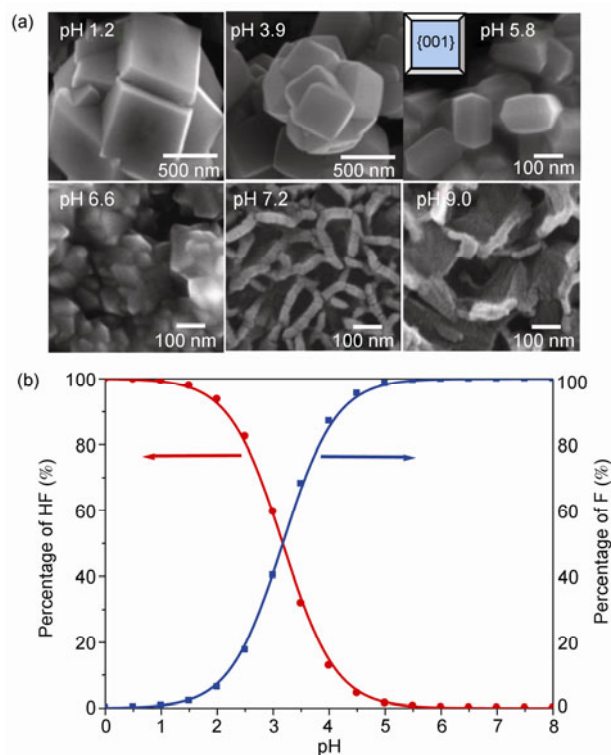

Figure 5 (a) SEM images of the hydrothermal products synthesized in HF reaction solution with different pH. Anatase TiO$_2$ microspheres with exposed {001} facets (pH 1.2 and 3.9); dispersed anatase TiO$_2$ single crystals with exposed {001} facets (pH 5.8); anatase TiO$_2$ nanoparticles with exposed {101} facets (pH 6.6); titanate nanorods and nanosheets (pH 7.2 and 9.0). (b) Effect of pH on 0.5% (v/v) HF solution speciation [57].

functional theory (DFT), the adsorption of HF or Na$^+$F$^-$ on the anatase TiO$_2$ (001) surface is calculated in the acidic or nearly neutral medium, respectively [57]. The adsorption strength is reflected by their adsorption energy (ΔE) based on the following equation:

$$\Delta E = E_{\text{tot}} - E_{\text{surf}} - E_{\text{ad}} \tag{1}$$

where E_{tot} and E_{surf} are the optimized total energies of systems with and without adsorbent, respectively, E_{ad} represents the energy of the optimized isolated HF or the energy per Na$^+$F$^-$ of the bulk crystal.

Figure 6 shows top view of HF/Na$^+$F$^-$ on an anatase TiO$_2$ (001) surface with the (8 × 4) surface cell based on DFT calculations. The results demonstrate that under acidic conditions, the dissociative adsorption of HF molecules on {001} faceted crystal surfaces is energetically permitted as demonstrated by the strong adsorption energy of −1.75 eV (Figure 6(A)). However, the interaction of Na$^+$F$^-$ with {001} faceted crystal surfaces is thermodynamically prohibited as shown by the calculated adsorption energy of +0.47 eV (Figure 6(B)) [57]. The higher bonding energy of O−H (−4.43 eV) versus O−Na (−2.65 eV) significantly contributes the dissociative adsorption of molecular form of HF on anatase TiO$_2$ (001) surfaces [57, 71]. To calculate the surface energies, the (1 × 1) surface cell with or without adsorbates on the both side of the slabs is employed. The surface energy (γ) is calculated by the following equation [72–75]:

$$\gamma = \frac{E_{\text{tot}} - NE_{\text{TiO}_2} - xE_{\text{ad}}}{2A} \tag{2}$$

where, E_{tot} is the total energy of the slab with or without adsorbates, N is the total number of unit TiO$_2$ contained in the slab model, E$_{\text{TiO2}}$ is the average energy per unit of TiO$_2$, x is the number of adsorbates in each cell, E_{ad} is the total energy of the isolated molecules of adsorbates, and A is the area of the (1 × 1) surface cell. When F (fluorine) atoms adsorb on the surface, E_{ad} is half of the total energy for F$_2$ [6]. In our study, the E_{ad} is the total energy for a HF (or F$_2$) molecule when HF molecules (F$_2$) adsorbs on the surface. The total energies for the isolated HF (or F$_2$) molecules are calculated in a big cubic box with the lattice constant as 15 Å.

Based on our calculation strategy, the surface energy of clean (001) surface of anatase TiO$_2$ is 0.92 J/m^2, which is close to the reported result by Lazzeri *et al.* (0.90 J/m^2) [76]. The surface energy of (001) surface of anatase TiO$_2$ is decreased to −0.50 J/m^2 after adsorbing HF molecules, which means that the adsorption of HF can facilitate the growth of the (001) surfaces, and effectively stabilize the grown (001) surfaces of anatase TiO$_2$. In our study, for comparison purpose, the surface energy of (001) surface of anatase TiO$_2$ is also calculated after adsorption of F$_2$ molecules using the same calculation strategy. The calculated value is −0.48
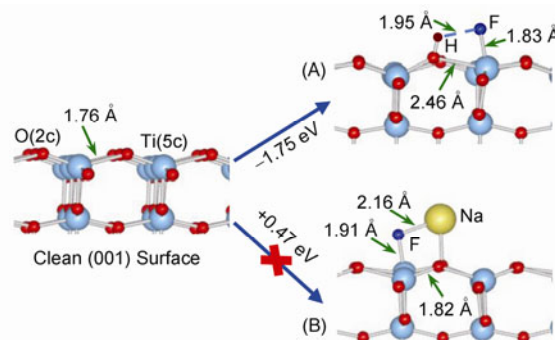

Figure 6   Top view of HF/Na$^+$F$^-$ on an anatase TiO$_2$ (001) surface with (8 × 4) surface cells. (A) The adsorption of HF; (B) the adsorption of Na$^+$F$^-$ [57].

J/m^2, which is slightly higher than the result reported by Yang et al. due to different calculation method [6]. The structural property studies of adsorbed surfaces also demonstrate that the interaction of HF molecules with (001) surface of anatase TiO$_2$ is remarkably stronger than that of Na$^+$F$^-$ with (001) surface, meaning that the preferential adsorption of HF on (001) surface of anatase TiO$_2$ [57].

Our theoretical and experimental studies confirmed that the {001} faceted anatase TiO$_2$ surface fluorination can occur only through dissociative adsorption of molecular form of HF under acidic conditions, and thus stabilizing and preserving {001} facets of anatase TiO$_2$ crystals.

3.3   Selective etching

Under surface fluorination concept, anatase TiO$_2$ crystals with exposed {001} facets have been widely reported since the pioneering work reported by Lu *et al*. [6]. The high reactive {001} facets of anatase TiO$_2$ have shown outstanding performance in photocatalytic, photoelectrocatalytic, solar energy conversion, hydrogen production, and lithium ion battery [7, 8, 12, 19, 39, 46, 47]. To date, all related reports have exclusively concluded that the surface fluorination of anatase TiO$_2$ can lower the {001} faceted surface energy, and thus preserving the grown {001} faceted surfaces. Very recently, we found experimentally that a selective etching on the {001} facets can occur under high HF concentration coditions [53]. This suggests that the reported mechanistic role of surface fluorination might be lopside. From the point of view of the control of crystal facet growth, this selective etching phenomenon can result in the crystal facet transformation from {001} to {101} (Figure 2(c,d)) [47]. Additionally, this self-etching ability can be also used to prepare nanoporous F-doped TiO$_2$ microspheres with visible light photocatalytic activity and anatase TiO$_2$ hollow microspherical photocatalyst for concurrent membrane water purifications [77, 78]. The results shown in Figure 7(a,b) demonstrate that anatase TiO$_2$ crystals with exposed and smooth {001} facets can be obtained from a reaction me-
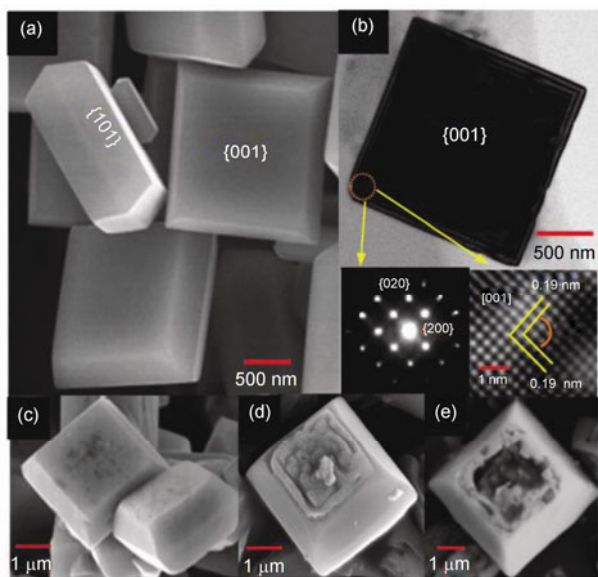
Figure 7   (a) SEM and (b) TEM images, and the corresponding SAED pattern and the HRTEM image of as-synthesized anatase TiO_2 single crystals fabricated from 4.5 mM TiF_4 aqueous solutions (pH 1.52); (c) to (e) SEM images of anatase TiO_2 single crystals fabricated in pH 1.52 aqueous solutions containing 5.2, 8.3, and 10.6 mM of TiF_4, respectively [53].

Figure 8   DFT calculated reaction energies and structures for different stages of HF interaction with single crystal anatase TiO_2 (101) (left) and (001) (right) surfaces. (a) Clean surfaces; (b) full HF-covered surfaces; (c) complete fluorinated surfaces; (d) etched surfaces. All structures are optimized structures [53].

Figure 9   The illustration of possible reactions of a partially HF-covered (001) surface ($\theta = 50\%$) under low HF concentrations. (a) Replacement of lattice O by F; (b) further adsorption of HF to the full coverage ($\theta = 100\%$). All structures are optimized structures [53].

dium containing 4.5 mM TiF_4 [53]. When the concentration of TiF_4 is beyond 5.2 mM, an eroded {001} faceted surface is observed, as shown in Figure 7(c,d) [53]. Almost entire {001} faceted surface is eroded with 10.6 mM TiF_4 (Figure 7(e)) [53]. Baed on these phenomena, one important concern is that why high concentration of HF can selectively destroy {001} facets?

To explain the etching mechanism of anatase TiO_2 {001} facets, we performed theoretical calculations based on DFT using Quantum Espresso software [79]. Based on our theoretical calculations, the dissociative adsorption of HF onto clean (101) and (001) surfaces (Figure 8(a)) is significantly initial step (Figure 8b) [53, 57]. Under the full coverage ($\theta = 100\%$) status, the DFT calculations indicate that the reaction energies of −2.49 eV and −2.56 eV for (101) and (001) surfaces, respectively, which means that the adsorption processes at both (101) and (001) surfaces are thermodynamically favorable [53]. Moreover, the surface exposed −OH group can be replaced by F with exothermic reaction energies of −0.73 eV and −1.20 eV for (101) and (001) surfaces, respectively, and thus resulting in a completely fluorinated surface under full coverage conditions (Figure 8(c)) [53]. Our calculations also demonstrate that the completely fluorinated crystal surfaces are covered by −$TiOF_2$. −$TiOF_2$ can be further dissolved from the crystal surfaces when the completely fluorinated crystal surfaces are exposed to a high concentrated HF, leading to a etched crystal surface (Figure 8d) [53]. In our study, the calculated dissolution reaction energies for (101) and (001) surfaces are −0.41 eV and +0.04 eV, respectively, which means that the
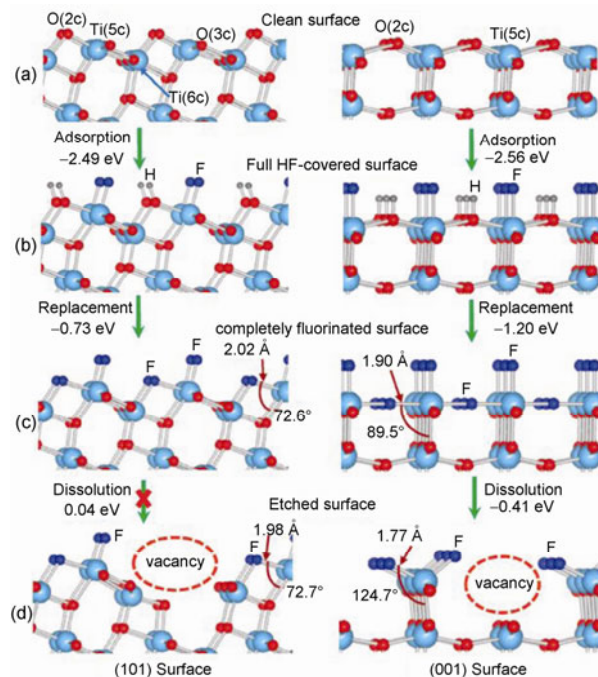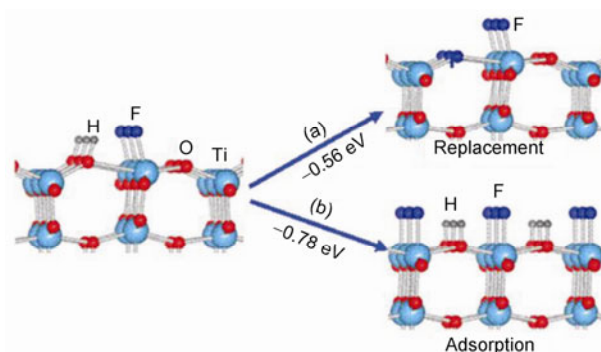
crystal surface etching is energetically permitted solely for the (001) surface [53]. The differences in the surface atomic structure arrangements for anatase TiO_2 (001) and (101) surfaces further explain the intrinsic reasons for the selective erosion phenomenon on {001} faceted surfaces under high HF concentration based on our theoretical calculation results [53].

Our theoretical calculations further explain why no surface etching takes place on anatase TiO_2 (001) surfaces under low concentrated HF solution (e.g., ≤ 4.5 mM), as shwon in Figure 9 [53]. With low concentrated HF, the (001)

cystal surfaces can be only partially covered by the adsorbed HF. The calculated results demonstrate that under partially HF coverage ($\theta = 50\%$), a further HF adsorption process to reach full coverage is 0.22 eV more energetically favored than that of the −OH group replacement process, which means that the −OH group replacement process can occur only after the full surface coverage status is achieved. Therefore, the etching phenomena on (001) facets cannot occur under low HF concentration. We believe that our studies provide a useful theoretical and practical guidance for controlled anatase TiO$_2$ crystal facets growth for more extensive applications.

4   Performance

Titanium dioxide (TiO$_2$) has been the dominant semiconductor material over the past two decades due to its potential applications in environmental remediation, solar energy conversion, biomedicine, and analytical determination of organic pollutants for water quality monitoring [26, 62, 80–87]. Controlled growth of anatase TiO$_2$ crystal facets with high reactivity is still pursued in the fields of science and technology owing to their superior intrinsic shape-independent properties in large numbers of applications. Since the pioneering work reported by Lu *et al*. [6], the synthesized anatase TiO$_2$ crystals with high reactive {001} facets have been applied in many fields such as photocatalysis [8, 88, 89], photoelectrocatalysis [47], solar energy conversion [7], hydrogen production [39], and lithium ion battery [12]. Recently, a α-Fe$_2$O$_3$/TiO$_2$ core/shell structured photocatalyst with magnetic function has been developed by Lou *et al*. [90]. The hollow composited material as photocatalyst possesses enhanced photocatalytic activity [90]. More strikingly, the photocatalyst can be readily recovered from the treated solution by applying a magnetic field due to its magnetic functionality [90]. Utilization of hydrofluoric acid (HF) strong etching peroperty, anatase mesoporous F-TiO$_2$ hollow microspheres have been used to construct filtration membrane, showing the multifunctions of concurrent photocatalytic degradation and membrane filtration for water purifications [78].

4.1   Photocatalytic activity

To date, most studies on anatase TiO$_2$ crystals with exposed {001} facets are exclusively formation of anatase TiO$_2$ crystals in solution suspension or precipitation forms [8, 11, 17, 18, 33, 34, 36–38, 41, 44, 46, 48, 60, 90–94]. After removal of fluorine by thermal treatment, clean anatase TiO$_2$ single crystals with 64% exposed {001} facets as photocatalysts exhibit superior photoreactivity (more than 5 times) compared to P25 TiO$_2$ as a benchmarking material for the degradation of terephthalic acid, as shown in Figure 10(a) [8]. Han *et al*. evaluated the photocatalytic performance of

anatase TiO$_2$ nanosheets with 89% exposed {001} facets using methyl orange (MO) as a probe substrate [18]. The experimental results indicated that the anatase nanosheets with exposed {001} facets possess higher photocatalytic activity than that of commercially available P25 TiO$_2$ (Figure 10(b)) [18]. Yu and co-workers have demonstrated that micrometer-sized anatase TiO$_2$ single crystals with 80% exposed {001} facets display much higher photocatalytic activities than that of the {001} unexposed TiO$_2$ single crystals (Figure 10(c)) [33]. They suggested that the high photocatalytic activities are mainly attributed to the strong ability of the reactive {001} facets to dissociatively adsorb water to form hydrogen peroxide and peroxide radicals [22, 33, 95, 96]. The anatase TiO$_2$ single crystals with exposed {001} and {110} high reactive facets obtained by a modified hydrothermal technique were evaluated by photocatalytic decolorization of MB dye under UV light irradiation [34]. In their study, the highest-surface-energy {110} facets were observed for the first time in the process of the growth of high reactive anatase TiO$_2$ {001} facets [34]. The results demonstrated that these anatase TiO$_2$ single crystals with high reactive {001} and {110} facets exhibit significantly enhanced photocatalytic efficiency for the decolorization of MB dye under UV light irradiation, as shown in Figure 10(d) [34].

Although anatase TiO$_2$ crystals with exposed {001} facets show high photocatalytic activities, these anatase crys-
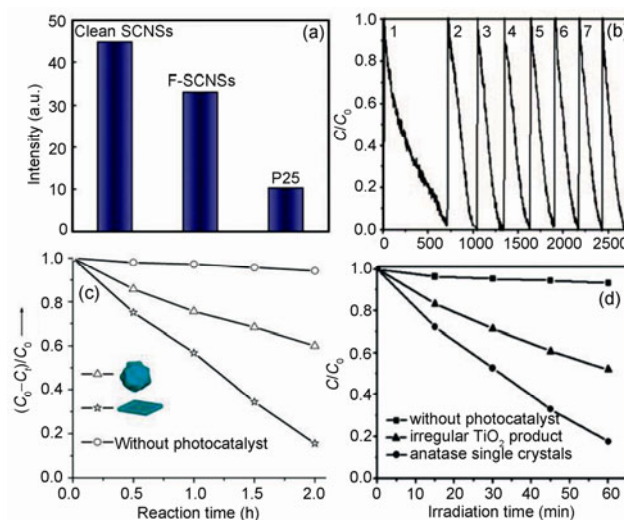

Figure 10   (a) Normalized fluorescence intensity per unit surface area with different photocatalysts: clean single crystal nanosheets with exposed {001} facets (SCNSs), TiO$_2$ SCNSs capped by F atoms (F-SCNSs), and Degussa P25 TiO$_2$; the photocatalytic reaction was performed in 3 mM terephthalic acid by Yang *et al*. [8]. (b) Cycling degradation curve for TiO$_2$ nanosheets (89% {001} facets) synthesized under the optimum reaction conditions, using 1 mmol/L MO as a probe by Han *et al*. [18]. (c) The effectiveness of samples with or without exposed reactive {001} facets on the degradation of 4-chlorophenol under UV irradiation reported by Yu *et al*. [33]. (d) The variation of MB concentration by photochemical reaction with the anatase TiO$_2$ single crystals and the irregular TiO$_2$ product by Liu *et al*. [34].

tals can be only used as photocatalysts for UV light utilization due to the large band gap (3.2 eV) of anatase TiO$_2$ [2]. Therefore, development of anatase TiO$_2$ crystals with exposed {001} facets and visible light activity has been highly desired for visible light utilization. To obtain visible light response, TiO$_2$ doped with metal and nonmetal elements has been extensively investigated in the past two decades [63, 97]. Very recently, Liu and co-workers have investigated nonmetal elements (i.g., N, S, B and I) doped anatase TiO$_2$ crystals with exposed {001} facets by simple hydrothermal methods [40, 41, 63, 98, 99]. These nonmetal elements doped anatase TiO$_2$ crystals with exposed {001} facets exhibit superior photocatalytic activities under visible light irradiation [40, 41, 63, 98, 99]. In their synthetic strategies, the undissolvable precursors such as TiN, TiS$_2$, and TiB$_2$ played key role in formation of visible light active anatase TiO$_2$ crystals with {001} facets [40, 41, 63, 98, 99].

Recently, anatase TiO$_2$ crystals with exposed {001} facets have been directly grown on metal titanium foil substrates using simple hydrothermal methods by our and other groups [47, 57, 100]. The anatase TiO$_2$ crystals grown on titanium foil substrates can offset the insufficiency of suspension or precipitation forms of anatase TiO$_2$ crystals with exposed {001} facets for more extensive applications such as photoelectrocatalysis and solar cells [30, 101–103]. Through controlling pH of HF reaction solution, we have developed different nanostructured photoelectrodes including anatase TiO$_2$ microspheres with exposed {001} facets and dispersed anatase TiO$_2$ nanocrystals with exposed {001} facets [47, 57]. The anatase TiO$_2$ microspheres with exposed {001} facets as photoelectrodes exhibited 1.5 times higher photocatalytic activity toward water oxidation than that of photoelectrodes composed of anatase TiO$_2$ microspheres with exposed {101} facets, as shown in Figure 11 [47]. This improved photoelectrocatalytic activity of anatase TiO$_2$ microsphere photoelectrode can be attributed to the higher oxidation ability of {001} facets compared to {101} facets [20]. Similarly, Wang *et al.* developed a facile hydrothermal route to directly grow TiO$_2$ films with oriented anatase {001} facets on titanium foil substrate [100]. After coating with CdS nanoparticles, the TiO$_2$ film with oriented {001} facets exhibited much improved photoelectrochemical water splitting performance [100]. The anatase TiO$_2$ crystals with exposed {001} facets directly grown on solide substrates extend undoubtedly their potential applications such as photoelectrocatalysis, solar energy conversion and lithium ion battery.

4.2   Dye-sensitized solar cells (DSSCs)

Since the pioneering work reported by O'Regan and Grätzel in 1991, anatase TiO$_2$ is still the preferred structure used in dye-sensitized solar cells (DSSCs) due to its larger bandgap (3.2 vs. 3.0 eV for rutile TiO$_2$) and higher conduction band edge energy, E_c [30, 81]. The higher conduction band edge
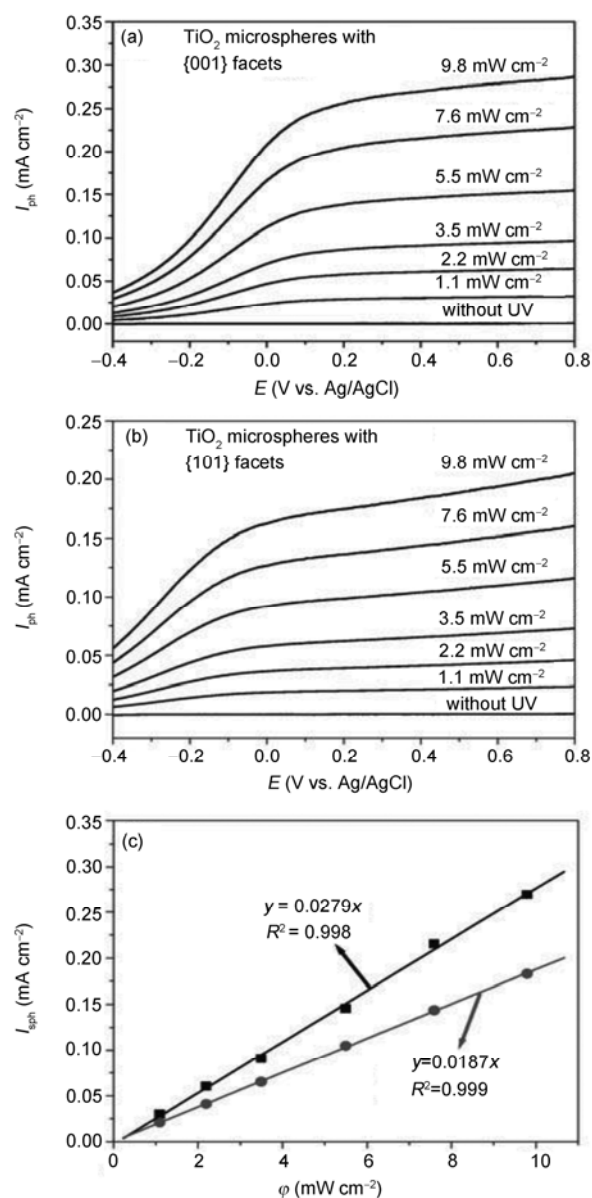

Figure 11   (a) Voltammograms of anatase TiO$_2$ photoelectrode fabricated from microspheres with exposed {001} facets at different UV light intensities. (b) Voltammograms of anatase TiO$_2$ photoelectrode fabricated from TiO$_2$ microspheres with {101} facets at different UV light intensities. (c) The relationships of saturation photocurrents for two anatase TiO$_2$ photoelectrodes and UV light intensities. The saturation photocurrents for two anatase TiO$_2$ photoelectrodes measured at +0.40 V and derived from Figure 11(a,b) [47].

energy of anatase TiO$_2$ can contribute higher Fermi level and open-circuit voltage (V_{oc}) in DSSCs for the same conduction band electron concentration [30]. To date, the reported anatase TiO$_2$ crystals with exposed {001} facets have exhibited superior photocatalytic activities [8, 18, 33, 50, 51]. These anatase TiO$_2$ crystals with high reactive facets are also highy attractive in DSSCs application [7, 21, 104].

In this respect, we have used anatase TiO$_2$ microspheres with exposed mirror-like plane {001} facets as light harvesting enhancement material in photoelectrode film con-

struction for DSSCs (Figure 12(a)) [7]. The resultant photoelectrodes with {001} facets dominated anatase TiO_2 microsphere light scattering top layer exhibited significantly improved light harvesting capability and overall light conversion efficiency (η = 7.91%), as shown in Figure 12(b) to (d) [7]. Our study demonstrated that the improved DSSCs efficiency is mainly due to the enhanced light scattering effect provided by the anatase TiO_2 microspheres with unique mirror-like plane {001} facets [7]. Besides the action of large size anatase TiO_2 microspheres, the improved DSSCs efficiency may be attributed to the unique mirror-like plane {001} facets with added ability to directly reflect the input light back to the bulk TiO_2 film, the effectiveness of the 400–600 nm square-shaped surface crystals for visible light scattering, and the enhanced effect by the layered configuration [7, 105–109]. Base on our study, the unique mirror-like plane {001} facets of anatase TiO_2 microspheres play important role in improving the light harvesting efficiency and DSSCs performance of the TiO_2 microsphere photoelectrodes. Similarly, anatase TiO_2 nanosheets-based hierarchical spheres with over 90% exposed {001} facets were used as photoanode material, showing a solar energy conversion efficiency of 7.51% [104]. Yu and co-workers reported recently that TiO_2 photoelectrodes made from anatase TiO_2 nanosheets with exposed {001} facets show importantly improved photoelectric conversion efficiency (η = 4.56%) in DSSCs in comparison with TiO_2 nanoparticle (η = 4.24%) and P25 photoelectrodes (η = 3.64%) [21]. Their study indicated that the

enhanced DSSCs performance is due to good crystallization, high pore volume, large particle size and improved light scattering effect of anatase TiO_2 nanosheets with exposed {001} facets in photoelectrode films [21].

4.3   Lithium ion battery

Development of high performance lithium ion battery has become a highly attractive research topic owing to its potential applications in electronic products and electrical vehicles [110–112]. As an electrode material, TiO_2 has been widely investigated in lithium ion battery because it is a low cost, abundant, structurally stable, and environmentally benign material [112–116]. Recently, hierarchical spheres made from large ultrathin anatase TiO_2 nanosheets with nearly 100% exposed {001} facets have been investigated in lithium ion battery by Lou and co-workers [12]. Their studies demonstrated that the high surface density of exposed {001} facets of anatase TiO_2 spheres results in fast lithium insertion/deinsertion processes in batteries, and thus high battery efficiency [12]. In their studies, the data of cyclic voltammograms showed that no apparent irreversible process was observed in the first cathodic scan, indicating a high Coulombic efficiency for lithium extraction, which is very unusual for anatase TiO_2 (Figure 13(a)) [12]. The charge-discharge profiles (Figure 13(b)) and reversibility measurements (Figure 13(c)) of the electrodes further demonstrated that the anatase TiO_2 hierarchical spheres made from large ultrathin nanosheets with nearly 100% exposed {001} facets possess excellent capacity retention and superior rate behavior in lithium ion batteries [12]. Lou and co-workers also investigated carbon and graphene-supported anatase TiO_2 nanosheets with exposed {001} facets for fast lithium storage [15, 16]. The results indicated that carbon-supported anatase TiO_2 nanosheets with exposed {001} facets show high reversible capacities with superior cyclic capacity retention at a high current rate [16]. The anatase TiO_2 nanosheets with exposed {001} facets significantly contribute the improved lithium storage performance due to the nanosheet structure allowing efficient lithium ion diffusion, as well as the effective nanocarbon support granting better structural stability [16]. The graphene-supported anatase TiO_2 nanosheets with exposed {001} facets also exhibited superior lithium storage performance [15]. This enhanced performance is mainly attributed to two factors: one is that the anatase TiO_2 nanosheets with exposed high reactive {001} facets can serve as ideal hosts for fast and efficient lithium storage; the other is that the graphene support can serve as a highly conductive substrate for high-rate electron transport [15]. In fact, the primary role of carbon and graphene in anatase TiO_2 nanosheet electrodes is to realize fast lithium ion diffusion, superior electron transport, and decreased resistance at the interface of electrode/electrolyte at high charge-discharge rates [117, 118].
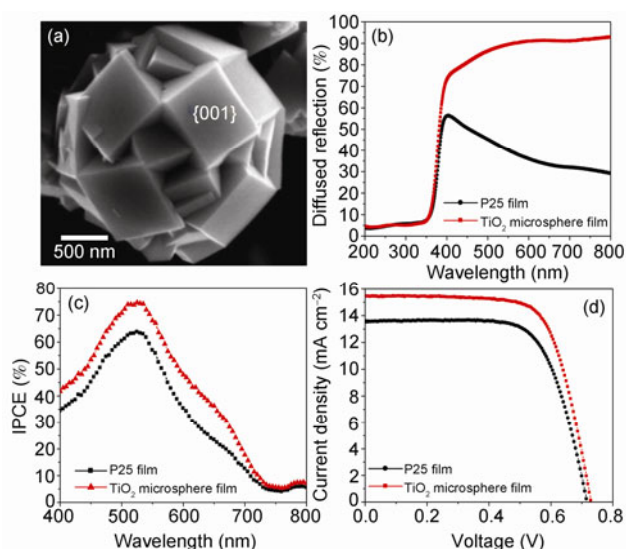

Figure 12   (a) High magnification SEM image of the as-synthesized anatase TiO_2 microspheres with exposed mirror-like plane {001} facets. (b) Diffuse reflectance spectra of the anatase TiO_2 microsphere and P25 films with similar thickness. (c) Incident photon to current conversion efficiency (IPCE) curves of the TiO_2 photoelectrode composing of TiO_2 microspheres with exposed mirror-like plane {001} facets and TiO_2 nanoparticles and the P25 photoelectrode. (d) Photocurrents as a function of photovoltage for DSSCs assembled with TiO_2 microsphere and P25 photoelectrodes [7].
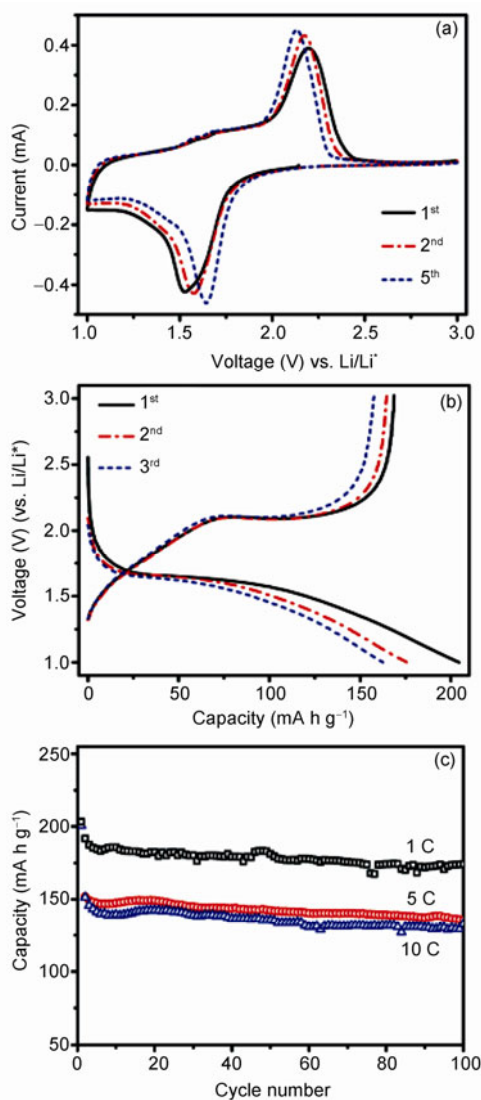
Figure 13 (a) Representative CVs at a scan rate of 0.2 mV/s for the first, second, and fifth cycles. (b) Charge-discharge profiles at a current rate of 5C (850 mA/g) for the first, second, and fifth cycles. (c) Cycling performance at different C rates. All of the measurements were conducted using a voltage window of 1.0–3.0 V reported by Lou *et al.* [12].

4.4 Hydrogen production

Since Fujishima and Honda's pioneering work in 1972, TiO_2 as an important functional material, has attracted great attention on water splitting for hydrogen production[26, 119–124]. Anatase TiO_2 crystals with exposed {001} facets are highly desired for hydrogen production by water splitting owing to their unique structure and high reactivity of {001} crystal facets [19, 39, 43, 50, 51]. Ultra-thin anatase TiO_2 nanosheets with various nanosheet thickness and percentage of {001} facets were used as photocatalysts loaded with 1 wt% of Pt for hydrogen evolution by water splitting [43]. The results demonstrated that corresponding to TiO_2 nanosheets with a thickness of 5.0, 2.7 and 1.6 nm, the hydrogen evolution rates are 4335, 7381 and 6958 µmol h^{-1}

g^{-1}, respectively [43]. The {001} faceted percentages of anatase TiO_2 nanosheets with a thickness of 5.0, 2.7 and 1.6 nm are 69%, 82% and 77%, respectively [43]. Their studies indicated that the highest rate of hydrogen production (7381 µmol h^{-1} g^{-1}) for anatase TiO_2 nanosheets with a thickness of 2.7 nm can be ascribed to their well-faceted morphology and high percentage (82%) of (001) reactive surface (Figure 14(a)) [43]. Yu *et al.* also investigated the rates of photocatalytic hydrogen production using Pt loaded anatase TiO_2 nanosheets with exposed {001} facets [39]. They found that the photocatalytic hydrogen production activity using the anatase TiO_2 nanosheets with exposed {001} facets can be significantly improved by loading Pt achieving the highest activity at Pt loading amount of 2% [39]. Their studies further indicated that all fluorinated TiO_2 nanosheets exhibit much higher photocatalytic hydrogen production activity than anatase TiO_2 nanosheets and pure TiO_2 nanoparticles without fluorination (Figure 14(b)) [39].
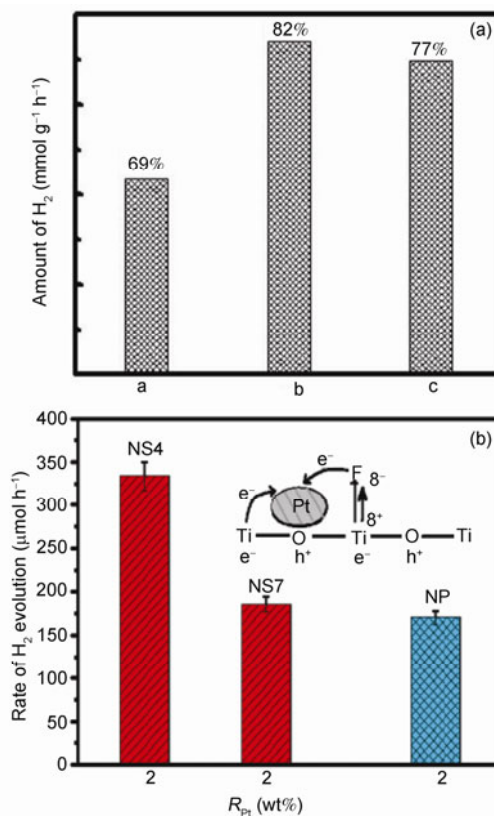

Figure 14 (a) Hydrogen evolution properties of the obtained TiO_2 nanosheets under UV-vis light irradiation. The percentages of {001} facets of anatase TiO_2 nanosheets are 69% (a), 82% (b) and 77% (c), respectively. The percentage of {001} facets of each sample is also illustrated on the top bars by Yang *et al.* [43]. (b) Comparison of the photocatalytic production of hydrogen from ethanol aqueous solutions for NS4 (nanosheets with F and R_{Pt} = 2), NS7 (nanosheets without F and R_{Pt} = 2), and NP (nanoparticles without F and R_{Pt} = 2). Inset shows the schematic diagram for generation and transfer of photogenerated e$^-$–h$^+$ pairs in F-TiO_2 under UV irradiation by Yu *et al.* [39].

4.5 Further discussion

Although many reports have demonstrated the superior photocatalytic activity of anatase TiO$_2$ crystals with exposed {001} facets, there are no direct evidences to make clear the reactivity of anatase TiO$_2$ {001} facets till recent studies reported by Pan et al. and Tachikawa *et al.* [19, 20]. Pan *et al*. compared the true photoreactivity order of {001}, {010}, and {101} facets of anatase TiO$_2$ crystals by comparing hydrogen evolution rate from water containing 10 vol% methanol using these anatase crystals with different exposed crystal facets [19]. The results indicated that for clean {001}, {101} and {010} facets, the photoreactivity order is of {001} < {101} < {010} for hydrogen evolution [19]. Furthermore, They performed theoretical calculations, UV-vis absorption spectra and X-ray photoelectron valence-band (VB) spectra measurements to prove and explain their conclusion. The results demonstrated that although VB maxima for three crystal facets dominated anatase TiO$_2$ crystals are at 1.93 eV (Figure 15(c)), the conduction-band (CB) minimum (Figure 15(d)) of {101} and {010} facets dominated anatase TiO$_2$ is obviously raised in contrast to {001} facets dominated anatase TiO$_2$ due to their slightly different band gaps (Figure 15(b,d)) [19]. Comparison with the {101} and {010} facets dominated anatase TiO$_2$, the more positive conduction-band edge potential of {001} facets dominated anatase TiO$_2$ is very disadvantageous for hydrogen generation [31], and thus leading to low hydrogen evolution rate [19]. In fact, based on Pan et al. work, a definite conclusion can be drawn: namely, the reduction capability of {101} and {010} facets dominated anatase TiO$_2$ crystals is higher than that of {001} facets dominated anatase TiO$_2$ crystals. This conclusion was further supported by a recent study reported by Tachikawa and co-workers [20].

In their studies, a single-molecule imaging and kinetic analysis of the fluorescence from the photocatalytic products on anatase TiO$_2$ crystal particles were used to compare the photoreactivity of the {101} and {001} crystal facets [20]. Their studies demonstrated that the reaction sites for the effective reduction of the probe molecules are preferentially located on the {101} crystal facets rather than the {001} crystal facets [20]. Figure 15(e) and (f) show fluorescence and transmission images of the same anatase TiO$_2$ crystal, respectively [20]. It can be clearly seen that the number of red dots (fluorescence bursts, Figure 15(f)) on (101) surface is nearly three times higher than the number of blue dots (fluorescence bursts, Figure 15(f)) on (001) surface, indicating that unique and important role of the (101) surface as the reductive site in photocatalysis [20]. Furthermore, they also investigated the oxidation reactivity of the {001} and {101} facets of individual TiO$_2$ crystal under UV irradiation using an oxidation-responsive fluorogenic probe [20]. The results demonstrated that the {001} facets of anatase TiO$_2$ crystals show a similar or slightly higher adsorption affinity and reactivity toward the amino-
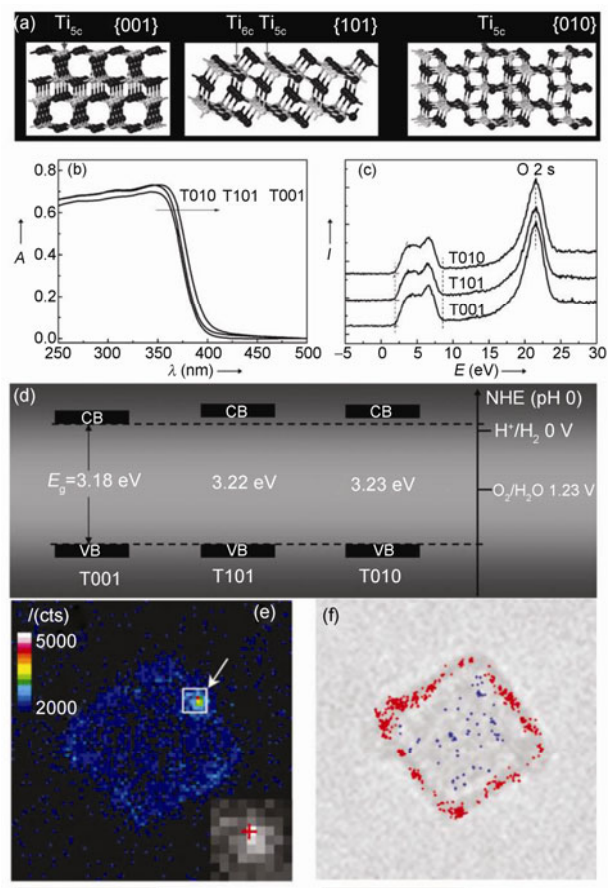

Figure 15 Surface atomic structure and electronic structure. (a) Schematic of the atomic structure of {001}, {101}, and {010} faces. (b) UV/Vis absorption spectra of T001, T101, and T010. (c) Valence-band XP spectra of T001, T101, and T010. d) Determined valence-band and conduction-band edges of T001, T101, and T010 by Pan *et al*. [19]. (e) Fluorescence and (f) transmission images of the same TiO$_2$ crystal immobilized on a cover glass in Ar-saturated methanol solution containing DN-BODIPY (2.0 μM) under a 488 nm laser and UV irradiation. The scale bars are 4 μm. The inset in Figure 15(e) shows the expanded image, as indicated by the arrow. The cross-mark shows the location of the reactive site. The blue and red dots in Figure 15(f) indicate the location of fluorescence bursts on the {001} and {101} facets of the crystal, respectively, observed during 3 min irradiation by Tachikawa *et al*. [20].

phenyl moiety of the probe than that of the {101} facets of anatase TiO$_2$ crystals [20]. These observations solve a fundamental question still arising on the photoreactivity of the {001} facets dominated anatase TiO$_2$ crystals, which provides a significant guide for synthesis of anatase TiO$_2$ crystals with desired crystal facets for more objective applications.

Based on the results reported by Pan *et al*. [19], {001} facets dominated anatase TiO$_2$ crystals possess more positive conduction band edge potential than that of {101} and {010} facets dominated anatase TiO$_2$ crystals, which is unfavored to reduce O$_2$ to O$_2^{\bullet-}$ during photocatalysis, and thus enhancing the recombination of photoelectron and hole [31]. As a powder form of photocatalyst, {001} facets dominated

anatase TiO$_2$ crystals with more positive conduction band edge potential (versus {101} and {010} facets dominated anatase TiO$_2$ crystals) could be very disadvantageous for photocatalytic oxidation of water and organics owing to high recombination of photoelectron and hole [31]. Because the oxidation capability of {001} facets dominated anatase TiO$_2$ crystals is importantly comparable with that of {101} and {010} facets dominated crystals [19, 20], therefore, this issue can be solved by a simple photoelectrochemical approach to decrease the recombination of photoelectron and hole [47, 57, 86, 87, 125–127]. Using this method, photo-generated electrons can be effectively transfer to external circuit by applying a potential bias, and thus significantly decreasing the recombination of photoelectron and hole and effectively improving the photocatalytic oxidation efficiency of photocatalyst [47, 57, 86, 87, 125–127]. However, the photocatalyst films immobilized on conducting substrates are necessary for use of this photoelectrochemical approach [47, 57, 86, 87, 125–127]. Therefore, fabrication of {001} facets dominated anatase TiO$_2$ crystals on conducting substrates is highly attractive for decreasing the recombination of photoelectron and hole and improving the photocatalytic oxidation efficiency by using this photoelectrocatalytic technique.

5   Summary and outlook

Controllable growth of anatase TiO$_2$ crystals with high reactive facets are highly desired in the fields of science and technology due to their unique structures and properties. Although the studies on anatase TiO$_2$ crystals with high reactive facets (e.g., {001} facets) have achieved fast development in recent few years, most studies are mainly focused on the development and improvement of the synthesized methods. Therefore, many challenges are still existent in the following several aspects: (1) Although theoretical calculations have demonstrated the critically important role of surface fluorination in growth of anatase TiO$_2$ crystals with exposed {001} facets, development of an environmental friendly synthetic system (without fluorine) is highly desired owing to the high toxicity and corrosive of fluorine-containing compounds. This requires theoretical and experimental workers pay more efforts to achieve it. (2) For anatase TiO$_2$, theoretical calculations have indicated that {101}, {001}, {010}, {100}, {103}, {105} and {107} crystal facets are possible during crystal growth [50]. However, most synthesized anatase TiO$_2$ crystals are dominated by {101} facets due to its low average surface energy. Therefore, combination with the theoretical calculations, development of the synthesized approaches to fabricate anatase TiO$_2$ crystals with other high reactive facets such as {103}, {105} and {107} facets is highly attractive for more extensive applications. Very recently, Yang *et al.* reported anatase TiO$_2$ crystals with exposed high-index {105} facets

fabricated by a modified high-temperature gas-phase oxidation route using titanium tetrachloride (TiCl$_4$) as precursor [128]. Such encouraging result suggests that synthesis of anatase TiO$_2$ with other exposed high reactive facets is achievable experimentally. (3) Based on the studies on anatase TiO$_2$ crystals with high reactive facets, synthesis of other metals or metal oxides with desirable crystal facets has considerably important significance for more extensive applications.

1   Gratzel M. Photoelectrochemical cells. *Nature*, 2001, 414: 338–344
2   Diebold U. The surface science of titanium dioxide. *Surf Sci Rep*, 2003, 48: 53–229
3   Tian N, Zhou Z-Y, Sun S-G, Ding Y, Wang ZL. Synthesis of tetrahexahedral platinum nanocrystals with high-index facets and high electro-oxidation activity. *Science*, 2007, 316: 732–735
4   Yin Y, Alivisatos AP. Colloidal nanocrystal synthesis and the organic-inorganic interface. *Nature*, 2005, 437: 664–670
5   Jun Y-W, Choi J-S, Cheon J. Shape control of semiconductor and metal oxide nanocrystals through nonhydrolytic colloidal routes. *Angew Chem Int Ed*, 2006, 45: 3414–3439
6   Yang HG, Sun CH, Qiao SZ, Zou J, Liu G, Smith SC, Cheng HM, Lu GQ. Anatase TiO$_2$ single crystals with a large percentage of reactive facets. *Nature*, 2008, 453: 638–641
7   Zhang H, Han Y, Liu X, Liu P, Yu H, Zhang S, Yao X, Zhao H. Anatase TiO$_2$ microspheres with exposed mirror-like plane {001} facets for high performance dye-sensitized solar cells (DSSCs). *Chem Commun*, 2010, 46: 8395–8397
8   Yang HG, Liu G, Qiao SZ, Sun CH, Jin YG, Smith SC, Zou J, Cheng HM, Lu GQ. Solvothermal synthesis and photoreactivity of anatase TiO$_2$ nanosheets with dominant {001} facets. *J Am Chem Soc*, 2009, 131: 4078–4083
9   Han X, Jin M, Xie S, Kuang Q, Jiang Z, Jiang Y, Xie Z, Zheng L. Synthesis of tin dioxide octahedral nanoparticles with exposed high-energy {221} facets and enhanced gas-sensing properties. *Angew Chem Int Ed*, 2009, 48: 9180–9183
10 Ma Y, Kuang Q, Jiang Z, Xie Z, Huang R, Zheng L. Synthesis of trioctahedral gold nanocrystals with exposed high-index facets by a facile chemical method. *Angew Chem Int Ed*, 2008, 47: 8901–8904
11 Wu B, Guo C, Zheng N, Xie Z, Stucky GD. Nonaqueous production of nanostructured anatase with high-energy facets. *J Am Chem Soc*, 2008, 130: 17563–17567
12 Chen JS, Tan YL, Li CM, Cheah YL, Luan D, Madhavi S, Boey Freddy YC, Archer LA, Lou XW. Constructing hierarchical spheres from large ultrathin anatase TiO$_2$ nanosheets with nearly 100% exposed (001) facets for fast reversible lithium storage. *J Am Chem Soc*, 2010, 132: 6124–6130
13 Chen JS, Luan D, Li CM, Boey FYC, Qiao S, Lou XW. TiO$_2$ and SnO$_2$@TiO$_2$ hollow spheres assembled from anatase TiO$_2$ nanosheets with enhanced lithium storage properties. *Chem Commun*, 2010, 46: 8252–8254
14 Ding S, Chen JS, Wang Z, Cheah YL, Madhavi S, Hu X, Lou XW. TiO$_2$ hollow spheres with large amount of exposed (001) facets for fast reversible lithium storage. *J Mater Chem*, 2010, 21: 1677–1680
15 Ding S, Chen JS, Luan D, Boey FYC, Madhavi S, Lou XW. Graphene-supported anatase TiO$_2$ nanosheets for fast lithium storage. *Chem Commun*, 2011, 47: 5780–5782
16 Chen JS, Liu H, Qiao SZ, Lou XW. Carbon-supported ultra-thin anatase TiO$_2$ nanosheets for fast reversible lithium storage. *J Mater Chem*, 2011, 21: 5687–5692
17 Liu G, Yang HG, Wang X, Cheng L, Pan J, Lu GQ, Cheng H-M.

Visible light responsive nitrogen doped anatase TiO$_2$ sheets with dominant {001} facets derived from TiN. *J Am Chem Soc*, 2009, 131: 12868–12869

18 Han X, Kuang Q, Jin M, Xie Z, Zheng L. Synthesis of titania nanosheets with a high percentage of exposed (001) facets and related photocatalytic properties. *J Am Chem Soc*, 2009, 131: 3152–3153

19 Pan J, Liu G, Lu GQ, Cheng H-M. On the true photoreactivity order of {001}, {010}, and {101} facets of anatase TiO$_2$ crystals. *Angew Chem Int Ed*, 2011, 50: 2133–2137

20 Tachikawa T, Yamashita S, Majima T. Evidence for crystal-face-dependent TiO$_2$ photocatalysis from single-molecule imaging and kinetic analysis. *J Am Chem Soc*, 2011, 133: 7197–7204

21 Yu J, Fan J, Lv K. Anatase TiO$_2$ nanosheets with exposed (001) facets: improved photoelectric conversion efficiency in dye-sensitized solar cells. *Nanoscale*, 2010, 2: 2144–2149

22 Selloni A. Crystal growth: Anatase shows its reactive side. *Nat Mater*, 2008, 7: 613–615

23 Wu X, Chen Z, Lu GQ, Wang L. Nanosized anatase TiO$_2$ single crystals with tunable exposed (001) facets for enhanced energy conversion efficiency of dye-sensitized solar cells. *Adv Funct Mater*, 2012, 21: 4167–4172

24 Sun L, Zhao Z, Zhou Y, Liu L. Anatase TiO$_2$ nanocrystals with exposed {001} facets on graphene sheets via molecular grafting for enhanced photocatalytic activity. *Nanoscale*, 2012, 4: 613–620

25 Liu B, Huang Y, Wen Y, Du L, Zeng W, Shi Y, Zhang F, Zhu G, Xu X, Wang Y. Highly dispersive {001} facets-exposed nanocrystalline TiO$_2$ on high quality graphene as a high performance photocatalyst. *J Mater Chem*, 2012, 22: 7484–7491

26 Fujishima A, Honda K. Electrochemical photolysis of water at a semiconductor electrode. *Nature*, 1972, 238: 37–38

27 Linsebigler AL, Lu G, Yates JT Jr. Photocatalysis on TiO$_2$ surfaces: Principles, mechanisms, and selected results. *Chem Rev*, 1995, 95: 735–758

28 Hagfeldt A, Graetzel M. Light-induced redox reactions in nanocrystalline systems. *Chem Rev*, 1995, 95: 49–68

29 Hoffmann MR, Martin ST, Choi W, Bahnemann DW. Environmental applications of semiconductor photocatalysis. *Chem Rev*, 1995, 95: 69–96

30 Hagfeldt A, Boschloo G, Sun L, Kloo L, Pettersson H. Dye-sensitized solar cells. *Chem Rev*, 2010, 110: 6595–6663

31 Fujishima A, Zhang X, Tryk DA. TiO$_2$ photocatalysis and related surface phenomena. *Surf Sci Rep*, 2008, 63: 515–582

32 Lazzeri M, Vittadini A, Selloni A. Structure and energetics of stoichiometric TiO$_2$ anatase surfaces. *Phys Rev B: Condens Matter Mater Phys*, 2002, 65: 119901/1

33 Zhang D, Li G, Yang X, Yu JC. A micrometer-size TiO$_2$ single-crystal photocatalyst with remarkable 80% level of reactive facets. *Chem Commun*, 2009, 4381–4383

34 Liu M, Piao L, Zhao L, Ju S, Yan Z, He T, Zhou C, Wang W. Anatase TiO$_2$ single crystals with exposed {001} and {110} facets: Facile synthesis and enhanced photocatalysis. *Chem Commun*, 2010, 46: 1664–1666

35 Alivov Y, Fan ZY. A method for fabrication of pyramid-shaped TiO$_2$ nanoparticles with a high {001} facet percentage. *J Phys Chem C*, 2009, 113: 12954–12957

36 Amano F, Prieto-Mahaney O-O, Terada Y, Yasumoto T, Shibayama T, Ohtani B. Decahedral single-crystalline particles of anatase titanium(IV) oxide with high photocatalytic activity. *Chem Mater*, 2009, 21: 2601–2603

37 Hu X, Zhang T, Jin Z, Huang S, Fang M, Wu Y, Zhang L. Single-crystalline anatase TiO$_2$ dous assembled micro-sphere and their photocatalytic activity. *Cryst Growth Des*, 2009, 9: 2324–2328

38 Xiang Q, Lv K, Yu J. Pivotal role of fluorine in enhanced photocatalytic activity of anatase TiO$_2$ nanosheets with dominant (001) facets for the photocatalytic degradation of acetone in air. *Appl Catal B*, 2010, 96: 557–564

39 Yu J, Qi L, Jaroniec M. Hydrogen production by photocatalytic water splitting over Pt/TiO$_2$ nanosheets with exposed (001) facets. *J Phys Chem C*, 2010, 114: 13118–13125

40 Liu G, Yang HG, Wang X, Cheng L, Pan J, Lu G, Qing M, Cheng H-M. Visible light responsive nitrogen doped anatase TiO$_2$ sheets with dominant {001} facets derived from TiN. *J Am Chem Soc*, 2009, 131: 12868–12869

41 Liu G, Yang H-G, Wang X-W, Cheng L, Lu H-F, Wang L-Z, Lu G-Q, Cheng H-M. Enhanced photoactivity of oxygen-deficient anatase TiO$_2$ sheets with dominant {001} facets. *J Phys Chem C*, 2009, 113: 21784–21788

42 Fang WQ, Zhou JZ, Liu J, Chen ZG, Yang C, Sun CH, Qian GR, Zou J, Qiao SZ, Yang HG. Hierarchical structures of single-crystalline anatase tio$_2$ nanosheets dominated by {001} facets. *Chem-Eur J*, 2011, 17: 1423–1427

43 Yang XH, Li Z, Liu G, Xing J, Sun C, Yang HG, Li C. Ultra-thin anatase TiO$_2$ nanosheets dominated with {001} facets. Thickness-controlled synthesis, growth mechanism and water-splitting properties. *CrystEngComm*, 2011, 13: 1378–1383

44 Yu H, Tian B, Zhang J. Layered TiO$_2$ composed of anatase nanosheets with exposed 001 facets: Facile synthesis and enhanced photocatalytic activity. *Chem-Eur J*, 2011, 17: 5499–5502

45 Yu J, Dai G, Xiang Q, Jaroniec M. Fabrication and enhanced visible-light photocatalytic activity of carbon self-doped TiO$_2$ sheets with exposed {001} facets. *J Mater Chem*, 2011, 21: 1049–1057

46 Zheng Z, Huang B, Qin X, Zhang X, Dai Y, Jiang M, Wang P, Whangbo M-H. Highly efficient photocatalyst: TiO$_2$ microspheres produced from TiO$_2$ nanosheets with a high percentage of reactive {001} facets. *Chem-Eur J*, 2009, 15: 12576–12579

47 Zhang H, Liu P, Li F, Liu H, Wang Y, Zhang S, Guo M, Cheng H, Zhao H. Facile Fabrication of anatase TiO$_2$ microspheres on solid substrates and surface crystal facet transformation from 001 to 101. *Chem-Eur J*, 2011, 17: 5949–5957

48 Xiang Q, Yu J, Jaroniec M. Tunable photocatalytic selectivity of TiO$_2$ films consisted of flower-like microspheres with exposed {001} facets. *Chem Commun*, 2011, 47: 4532–4534

49 Liu S, Yu J, Jaroniec M. Tunable photocatalytic selectivity of hollow TiO$_2$ microspheres composed of anatase polyhedra with exposed {001} facets. *J Am Chem Soc* 132: 11914–11916

50 Wen CZ, Jiang HB, Qiao SZ, Yang HG, Lu GQ. Synthesis of high-reactive facets dominated anatase TiO$_2$. *J Mater Chem*, 2011, 21: 7052–7061

51 Fang WQ, Gong X-Q, Yang HG. On the unusual properties of anatase TiO$_2$ exposed by highly reactive facets. *J Phys Chem Lett*, 2011, 2: 725–734

52 Liu G, Yu JC, Lu GQ, Cheng HM. Crystal facet engineering of semiconductor photocatalysts: motivations, advances and unique properties. *Chem. Commun* 2011, 47: 6763–6783

53 Wang Y, Zhang H, Han Y, Liu P, Yao X, Zhao H. A selective etching phenomenon on {001} faceted anatase titanium dioxide single crystal surfaces by hydrofluoric acid. *Chem Commun*, 2011, 47: 2829–2831

54 Wang X, Huang B, Wang Z, Qin X, Zhang X, Dai Y, Whangbo M-H. Synthesis of anatase TiO$_2$ tubular structures microcrystallites with a high percentage of {001} facets by a simple one-step hydrothermal template process. *Chem-Eur J*, 2010, 16: 7106–7109

55 Wang Z, Huang B, Dai Y, Zhang X, Qin X, Li Z, Zheng Z, Cheng H, Guo L. Topotactic transformation of single-crystalline TiOF$_2$ nanocubes to ordered arranged 3D hierarchical TiO$_2$ nanoboxes. *CrystEngComm*, 2012, 14: 4578–4581

56 Zhu J, Wang S, Bian Z, Xie S, Cai C, Wang J, Yang H, Li H. Solvothermally controllable synthesis of anatase TiO$_2$ nanocrystals with dominant {001} facets and enhanced photocatalytic activity. *CrystEngComm*, 2010, 12: 2219–2224

57 Zhang H, Wang Y, Liu P, Han Y, Yao X, Zou J, Cheng HM, Zhao H. Anatase TiO$_2$ crystal facet growth: Mechanistic role of hydrofluoric acid and photoelectrocatalytic activity. *ACS Appl Mater Interf*, 2011, 3: 2472–2478

58 Wen CZ, Zhou JZ, Jiang HB, Hu QH, Qiao SZ, Yang HG. Synthesis of micro-sized titanium dioxide nanosheets wholly exposed with high-energy {001} and {100} facets. *Chem Commun*, 2011, 47: 4400–4402

59 Dai Y, Cobley CM, Zeng J, Sun Y, Xia Y. Synthesis of anatase TiO₂ nanocrystals with exposed {001} facets. *Nano Lett*, 2009, 9: 2455–2459

60 Liu G, Sun C, Yang HG, Smith SC, Wang L, Lu GQ, Cheng H-M. Nanosized anatase TiO₂ single crystals for enhanced photocatalytic activity. *Chem Commun*, 2010, 46: 755–757

61 Hashimoto K, Irie H, Fujishima A. TiO₂ photocatalysis: A historical overview and future prospects. *Jpn J Appl Phys, Part 1*, 2005, 44: 8269–8285

62 Mills A, Le Hunte S. An overview of semiconductor photocatalysis. *J Photochem Photobiol, A*, 1997, 108: 1–35

63 Liu G, Wang L, Yang HG, Cheng H-M, Lu GQ. Titania-based photocatalysts-crystal growth, doping and heterostructuring. *J Mater Chem*, 2010, 20: 831–843

64 Bikondoa O, Pang CL, Ithnin R, Muryn CA, Onishi H, Thornton G. Direct visualization of defect-mediated dissociation of water on TiO₂(110). *Nat Mater*, 2006, 5: 189–192

65 Dulub O, Batzilln M, Solovev S, Loginova E, Alchagirov A, Madey TE, Diebold U. Electron-induced oxygen desorption from the TiO₂(011)-2x1 surface leads to self-organized vacancies. *Science*, 2007, 317: 1052–1056

66 Gong X-Q, Selloni A, Batzill M, Diebold U. Steps on anatase TiO₂(101). *Nat Mater*, 2006, 5: 665–670

67 Barnard AS, Curtiss LA. Prediction of TiO₂ nanoparticle phase and shape transitions controlled by surface chemistry. *Nano Lett*, 2005, 5: 1261–1266

68 Sun C-H, Liu L-M, Selloni A, Lu GQ, Smith SC. Titania-water interactions: a review of theoretical studies. *J Mater Chem*, 2010, 20: 10319–10334

69 Kavan L, Graetzel M, Gilbert SE, Klemenz C, Scheel HJ. Electrochemical and photoelectrochemical investigation of single-crystal anatase. *J Am Chem Soc*, 1996, 118: 6716–6723

70 Zmbov KF, Margrave JL. Mass spectrometric studies at high temperatures. XVI. Sublimation pressures for titanium(III)fluoride and the stabilities of TiF2(g) and TiF(g). *J Phys Chem*, 1967, 71: 2893–2895

71 Anon, *CRC Handbook of Chemistry and Physics. 81st Edition. Edited by David R. Lide (National Institute of Standards and Technology)*. Boca Raton, FL: CRC Press, 2000, 122: 12614

72 Barnard AS, Zapol P. Effects of particle morphology and surface hydrogenation on the phase stability of TiO₂. *Phys Rev B: Condens Matter Mater Phys*, 2004, 70: 235403/1-235403/13

73 Barnard AS, Zapol P, Curtiss LA. Anatase and rutile surfaces with adsorbates representative of acidic and basic conditions. *Surf Sci*, 2005, 582: 173–188

74 Wang X-G, Chaka A, Scheffler M. Effect of the environment on alpha-Al₂O₃ (0001) surface structures. *Phys Rev Lett*, 2000, 84: 3650–3653

75 Reuter K, Scheffler M. Composition, structure, and stability of RuO₂(110) as a function of oxygen pressure. *Phys Rev B: Condens Matter Mater Phys*, 2002, 65: 035406/1-035406/11

76 Lazzeri M, Vittadini A, Selloni A. Structure and energetics of stoichiometric TiO₂ anatase surfaces. *Phys Rev B: Condens Matter Mater Phys*, 2001, 63: 155409/1-155409/9

77 Ho W, Yu JC, Lee S. Synthesis of hierarchical nanoporous F-doped TiO₂ spheres with visible light photocatalytic activity. *Chem Commun*, 2006, 1115–1117

78 Pan JH, Zhang X, Du AJ, Sun DD, Leckie JO. Self-etching reconstruction of hierarchically mesoporous F-TiO₂ hollow microspherical photocatalyst for concurrent membrane water purifications. *J Am Chem Soc*, 2008, 130: 11256–11257

79 Giannozzi P, Baroni S, Bonini N, Calandra M, Car R, Cavazzoni C, Ceresoli D, Chiarotti GL, Cococcioni M, Dabo I, Dal Corso A, De Gironcoli S, Gebauer R, Gerstmann U, Gougoussis C, Kokalj A, Lazzeri M, Colomer LMS, Marzari N, Mauri F, Paolini S, Pasquarello A, Paulatto L, Sbraccia C, Scandolo S, Sclauzero G, Seitsonen AP, Smogunov A, Umari P, Wentzcovitch RM. QUANTUM ESPRESSO: a modular and open-source software project for quantum simulations of materials. *arXiv.org, e-Print Arch, Condens Matter*, 2009, 1–18

80 Burda C, Chen X, Narayanan R, El-Sayed MA. Chemistry and properties of nanocrystals of different shapes. *Chem Rev*, 2005, 105: 1025–1102

81 O'regan B, Graetzel M. A low-cost, high-efficiency solar cell based on dye-sensitized colloidal titanium dioxide films. *Nature*, 1991, 353: 737–740

82 Ghicov A, Schmuki P. Self-ordering electrochemistry: a review on growth and functionality of TiO₂ nanotubes and other self-aligned MOx structures. *Chem Commun*, 2009, 20: 2791–2808

83 Mor GK, Varghese OK, Paulose M, Shankar K, Grimes CA. A review on highly ordered, vertically oriented TiO₂ nanotube arrays: Fabrication, material properties, and solar energy applications. *Sol Energy Mater Sol Cells*, 2006, 90: 2011–2075

84 Song Y-Y, Schmidt-Stein F, Bauer S, Schmuki P. Amphiphilic TiO₂ nanotube arrays: An actively controllable drug delivery system. *J Am Chem Soc*, 2009, 131: 4230–4232

85 Zhang H, Liu P, Liu X, Zhang S, Yao X, An T, Amal R, Zhao H. Fabrication of highly ordered TiO₂ nanorod/nanotube adjacent arrays for photoelectrochemical applications. *Langmuir*, 2010, 26: 11226–11232

86 Zhao H, Jiang D, Zhang S, Catterall K, John R. Development of a direct photoelectrochemical method for determination of chemical oxygen demand. *Anal Chem*, 2004, 76: 155–160

87 Zhang S, Jiang D, Zhao H Development of chemical oxygen demand on-line monitoring system based on a photoelectrochemical degradation principle. *Environ Sci Technol*, 2006. 40: 2363–2368

88 Wang Z, Huang B, Dai Y, Liu Y, Zhang X, Qin X, Wang J, Zheng Z, Cheng H. Crystal facets controlled synthesis of graphene@TiO₂ nanocomposites by a one-pot hydrothermal process. *CrystEngComm*, 2012, 14: 1687–1692

89 Zheng Z, Huang B, Lu J, Qin X, Zhang X, Dai Y. Hierarchical TiO₂ microspheres: synergetic effect of {001} and {101} facets for enhanced photocatalytic activity. *Chem-Eur J*, 2011, 17: 15032–15038

90 Chen J-S, Chen C-P, Liu J, Xu R, Qiao S-Z, Lou X-W. Ellipsoidal hollow nanostructures assembled from anatase TiO₂ nanosheets as a magnetically separable photocatalyst. *Chem Commun*, 2011, 47: 2631–2633

91 Amano F, Yasumoto T, Mahaney OOP, Uchida S, Shibayama T, Terada Y, Ohtani B. Highly active titania photocatalyst particles of controlled crystal phase, size, and polyhedral shapes. *Top Catal*, 2010, 53: 455–461

92 Cao F-L, Wang J-G, Lv F-J, Zhang D-Q, Huo Y-N, Li G-S, Li H-X, Zhu J. Photocatalytic oxidation of toluene to benzaldehyde over anatase TiO₂ hollow spheres with exposed {001} facets. *Catal Commun*, 2011, 12: 946–950

93 Liu G, Sun C, Yang HG, Smith SC, Wang L, Lu GQ, Cheng H-M. Nanosized anatase TiO₂ single crystals for enhanced photocatalytic activity. *Chem Commun*, 2010, 46: 755–757

94 Zhou JK, Lv L, Yu J, Li HL, Guo P-Z, Sun H, Zhao XS. Synthesis of self-organized polycrystalline F-doped TiO₂ hollow microspheres and their photocatalytic activity under visible light. *J Phys Chem C*, 2008, 112: 5316–5321

95 Gong X-Q, Selloni A. Reactivity of anatase TiO₂ nanoparticles: the role of the minority (001) surface. *J Phys Chem B*, 2005, 109: 19560–19562

96 Bredow T, Jug K. SINDO1 Study of photocatalytic formation and reactions of OH radicals at anatase particles. *J Phys Chem*, 1995, 99: 285–291

97 Zaleska A. Doped-TiO₂: A review. *Recent Pat Eng*, 2008, 2: 157–164

98 Liu G, Sun C, Smith SC, Wang L, Lu GQ, Cheng H-M. Sulfur doped anatase TiO₂ single crystals with a high percentage of {001} facets. *J Colloid Interface Sci*, 2010, 349: 477–483

99 Liu G, Sun C, Yan X, Cheng L, Chen Z, Wang X, Wang L, Smith SC, Lu GQ, Cheng H-M. Iodine doped anatase TiO₂ photocatalyst with ultra-long visible light response: correlation between geometric/electronic structures and mechanisms. *J Mater Chem*, 2009, 19: 2822–2829

100 Wang X-W, Liu G, Wang L-Z, Pan J, Lu GQ, Cheng H-M. TiO₂

films with oriented anatase {001} facets and their photoelectrochemical behavior as CdS nanoparticle sensitized photoanodes. *J Mater Chem*, 2011, 21: 869–873

101 Shankar K, Basham JI, Allam NK, Varghese O, Mor GK, Feng X, Paulose M, Seabold JA, Choi K-S, Grimes CA. Recent advances in the use of TiO₂ nanotube and nanowire arrays for oxidative photoelectrochemistry. *J Phys Chem C*, 2009, 113: 6327–6359

102 Miyasaka T. Toward printable sensitized mesoscopic solar cells: Light-harvesting management with thin TiO₂ films. *J Phys Chem Lett*, 2011, 2: 262–269

103 Preat J, Jacquemin D, Perpete EA. Towards new efficient dye-sensitised solar cells. *Energy Environ Sci*, 2010, 3: 891–904

104 Yang W, Li J, Wang Y, Zhu F, Shi W, Wan F, Xu D. A facile synthesis of anatase TiO₂ nanosheets-based hierarchical spheres with over 90% {001} facets for dye-sensitized solar cells. *Chem Commun*, 2011, 47: 1809–1811

105 Huang F, Chen D, Zhang XL, Caruso RA, Cheng Y-B. Dual-function scattering layer of submicrometer-sized mesoporous tio₂ beads for high-efficiency dye-sensitized solar cells. *Adv Funct Mater*, 2010, 20: 1301–1305

106 Chen D, Huang F, Cheng Y-B, Caruso RA. Mesoporous anatase TiO₂ beads with high surface areas and controllable pore sizes: A Superior candidate for high-performance dye-sensitized solar cells. *Adv Mater*, 2009, 21: 2206–2210

107 Sauvage F, Chen D, Comte P, Huang F, Heiniger L-P, Cheng Y-B, Caruso RA, Graetzel M. Dye-sensitized solar cells employing a single film of mesoporous TiO₂ beads achieve power conversion efficiencies over 10%. *ACS Nano*, 2010, 4: 4420–4425

108 Zhang Q, Dandeneau CS, Zhou X, Cao G. ZnO Nanostructures for dye-sensitized solar cells. *Adv Mater*, 2009, 21: 4087–4108

109 Zhang Q, Dandeneau CS, Park K, Liu D, Zhou X, Jeong Y-H, Cao G. Light scattering with oxide nanocrystallite aggregates for dye-sensitized solar cell application. *J Nanophotonics*, 2010, 4: 1–23

110 Arico AS, Bruce P, Scrosati B, Tarascon J-M, Van Schalkwijk W. Nanostructured materials for advanced energy conversion and storage devices. *Nat Mater*, 2005, 4: 366–377

111 Kang B, Ceder G. Battery materials for ultrafast charging and discharging. *Nature*, 2009, 458: 190–193

112 Wang D, Choi D, Li J, Yang Z, Nie Z, Kou R, Hu D, Wang C, Saraf LV, Zhang J, Aksay IA, Liu J. Self-assembled TiO₂-graphene hybrid nanostructures for enhanced Li-ion insertion. *ACS Nano*, 2009, 3: 907–914

113 Li J, Wan W, Zhou H, Li J, Xu D. Hydrothermal synthesis of TiO₂(B) nanowires with ultrahigh surface area and their fast charging and discharging properties in Li-ion batteries. *Chem Commun*, 2011, 47: 3439–3441

114 Li N, Liu G, Zhen C, Li F, Zhang L, Cheng H-M. Battery performance and photocatalytic activity of mesoporous anatase TiO₂ nanospheres/graphene composites by template-free self-assembly. *Adv Funct Mater*, 2011, 21: 1717–1722

115 Park K-S, Kang J-G, Choi Y-J, Lee S, Kim D-W, Park J-G. Long-term, high-rate lithium storage capabilities of TiO₂ nanostructured electrodes using 3D self-supported indium tin oxide conducting nanowire arrays. *Energy Environ Sci*, 2011, 4: 1796–1801

116 Xue L, Wei Z, Li R, Liu J, Huang T, Yu A. Design and synthesis of Cu₆Sn₅-coated TiO₂ nanotube arrays as anode material for lithium ion batteries. *J Mater Chem*, 2011, 21: 3216–3220

117 Maier J. Nanoionics: Ion transport and electrochemical storage in confined systems. *Nat Mater*, 2005, 4: 805–815

118 Tarascon JM, Armand M. Issues and challenges facing rechargeable lithium batteries. *Nature*, 2001, 414: 359–367

119 Roy P, Das C, Lee K, Hahn R, Ruff T, Moll M, Schmuki P. Oxide nanotubes on Ti-Ru alloys: Strongly enhanced and stable photoelectrochemical activity for water splitting. *J Am Chem Soc*, 2011, 133: 5629–5631

120 Mor GK, Shankar K, Paulose M, Varghese OK, Grimes CA. Enhanced photocleavage of water using titania nanotube arrays. *Nano Lett*, 2005, 5: 191–195

121 Mor GK, Varghese OK, Wilke RHT, Sharma S, Shankar K, Latempa TJ, Choi K-S, Grimes CA. p-Type Cu-Ti-O nanotube arrays and their use in self-biased heterojunction photoelectrochemical diodes for hydrogen generation. *Nano Lett*, 2008, 8: 1906–1911

122 Chen X, Liu L, Yu PY, Mao SS. Increasing solar absorption for photocatalysis with black hydrogenated titanium dioxide nanocrystals. *Science*, 2011, 331: 746–750

123 Chen J-J, Wu JCS, Wu PC, Tsai DP. Plasmonic photocatalyst for H₂ evolution in photocatalytic water splitting. *J Phys Chem C*, 2011, 115: 210–216

124 Alenzi N, Liao W-S, Cremer PS, Sanchez-Torres V, Wood TK, Ehlig-Economides C, Cheng Z. Photoelectrochemical hydrogen production from water/methanol decomposition using Ag/TiO₂ nanocomposite thin films. *Int J Hydrogen Energy*, 2010, 35: 11768–11775

125 Zhang H, Zhao H, Zhang S, Quan X. Photoelectrochemical manifestation of photoelectron transport properties of vertically aligned nanotubular TiO₂ photoanodes. *ChemPhysChem*, 2008, 9: 117–123

126 Zhao H, Shen Y, Zhang S, Zhang H. A vapor phase hydrothermal modification method converting a honeycomb structured hybrid film into photoactive TiO₂ film. *Langmuir*, 2009, 25: 11032–11037

127 Jiang D, Zhao H, Zhang S, John R. Characterization of photoelectrocatalytic processes at nanoporous TiO₂ film electrodes: photocatalytic oxidation of glucose. *J Phys Chem B*, 2003, 107: 12774–12780

128 Jiang HB, Qian C, Wen CZ, Xing J, Wu D, Gong X-Q, Li C, Yang HG. Anatase TiO₂ crystals with exposed high-index facets. *Angew Chem Int Ed*, 2011, 50: 3764–3768